Int. J. Electrochem. Sci., 14 **(2019)** 6976 – 6985, doi; 10.20964/2019.07.79

International Journal of
ELECTROCHEMICAL
SCIENCE
www.electrochemsci.org

Controlling the Structure and Electrochemical Properties of Anode Prepared from Phenolic Resin for Li-ion Batteries

Zan Zhou[1], *Zhiqiang Gu*[1], *Yuede He*[1*], *Dachun Peng*[1], *Chenguang Bao*[1], *Hongbo Liu*[1, 2**]

[1] College of Materials Science and Engineering, Hunan University, Changsha, China
[2] Hunan Province Key Laboratory for Advanced Carbon Materials and Applied Technology, Hunan University, Changsha, Hunan, 410082, China
[*]E-mail: heyuede@163.com (Yuede He); hndxlhb@163.com (Hongbo Liu);

Received: 14 March 2019 / *Accepted:* 2 May 2019 / *Published:* 10 June 2019

The type and molecular weight of precursor has significant influence on the structural characteristics and electrochemical performances of hard carbon which derived from phenolic resins. A series of hard carbon samples have been prepared by carbonization treatment of Novolak and Resole with different molecular weight under vacuum. Take advantage of the large layer spacing, more defects and unique pores distribution of the hard carbon that prepared from Resole with low molecular weight, which exhibits an excellent reversible capacity of 606 mA h g^{-1} and a superior rate performance.

Keywords: hard carbon; Lithium-ion batteries; phenolic resin; molecular weight; anode

1.INTRODUCTION

Since the commercialization application of Lithium-ion batteries(LIBs) in early 1990s, LIBs have been widely applied in portable devices, electric vehicles (EVs) and hybrid electric vehicles (HEVs) due to their advantages such as high energy density, long cycling life, slow self-discharge and no memory effect. Graphite anode is the mostly used anode in LIBs, owing to the great cycling performance, low working potential and low-cost, so far. However, graphite anode suffers from low capacity (372 mA h g^{-1}) and low rate performance, which have restricted its application for high performance EVs and HEVs. It is urgent to seek alternative anode materials with high capacity and great rate performance. Hard carbon (HC) is a kind of carbonaceous materials, which has been

developed for application as LIB anode. From the viewpoint of structure, HC is a type of non-graphitizing carbon with highly irregular structure consisting of many tiny graphene sheets and only a few layers stacked in disorder. Recently, many studies on the application of HC as LIB anode materials have been reported. Attributing to the special structure, HC anodes possess more active sites to store lithium ion compare with graphite, including both sides of the carbon sheets, carbon sheet edges, micropores formed from the random stacking of graphitic crystallites, and atomic defect. It is possible to achieve a higher theoretical capacity (500-700 mA h g^{-1}), which is twice the capacity of graphite anode [1–4]. Generally speaking, the amount of extra insertion has direct connected with the ratio of single graphene sheets and the amount of defect [5]. Weibing Xing [6] explored the relationship between the capacity of lithium ion intercalation and the HC microstructure, they found that the capacity of HC intercalation is related to the pore size of the micropores and the (002) peak intensity. Moreover, the interlayer spacing between carbon sheets is larger than that of graphite sheets, which is beneficial to the diffusion of lithium ions in HC anode materials. As a result, the HC has high capacity and rate performance, which may be more suitable for electric vehicles and hybrid electric vehicles. Additionally, an importance advantage of commercial application of hard carbon is the abundant source of precursor, which can be prepared from different precursor materials such as polymers [7–9], biomass materials [10–13], and bacterial [14–16]. In particular, phenolic resin-based HCs have received great attention owing to its advantages such as simple prepared process, low cost, and high carbon yield.

The aim of the study is to investigate the effect of the molecular weight and type of phenolic resin on the structural and electrochemical performances of HCs. In this work, we using Novolak-type and Resole-type phenolic resin as precursors to prepare hard carbon, a series of HCs derived from phenolic resin with different molecular weight have been prepared under the same experimental process. It is revealed that the molecular weight of phenolic resin could affect the value of d_{002} and *ID/IG* of HCs, and the electrochemical performances of HCs are significantly related to the value of d_{002} and *ID/IG*. The HC anode with a higher value of d_{002} and *ID/IG*, delivered an outstanding reversible capacity, rate performance, cyclic performance as well as initial coulombic efficiency.

2. EXPERIMENTAL

2.1. Materials

Hexamethylenetetramine (AR, sinopharm) dissolved in DI water was prepared as the hardener. The phenolic resin used in the study was obtained from SUMITOMO BAKELITE (NANTONG) CO.LTD. As hard carbon precursor, middle molecular weight Novolak-type phenolic resin(MNR; Mn=519), high molecular weight Novolak resin(HNR; Mn=721), low molecular weight Resole-type phenolic resin (LRR; Mn=282), middle molecular weight Resole-type phenolic resin (MRR; Mn=870) and high molecular weight Resole-type phenolic resin (HRR; Mn=951) were dissolved in Ethanol or DMF (HRR is insoluble in ethanol, but easy to DMF) at a concentration of 10 wt.%. Each phenolic resin solution was blended with the HMTA solution and cured in air at 180 ℃ for 6 h.

These cured precursors were heated from room temperature to 500 ℃ maintained 2 h, and then heated at 800 ℃ under vacuum (100 Pa) for 6 h with ramp rate of 5 ℃ min^{-1}. After cooling down under Nitrogen atmosphere, the hard carbon was ground and shifted to 325 mesh to obtained the negative materials.

According to their molecular weight (the abbreviations of low molecular weight, middle molecular weight and high molecular weight are L, M and H respectively) and type (the abbreviations of Novolak and Resole are N and R respectively.), the.as-prepared hard carbons were named as MNHC, HNHC, LRHC, MRHC and HRHC, respectively.

2.2. Characterizations

The morphologies of HCs were observed through scanning electron microscopy (SEM, Hitachi S-4800, Japan). X-ray diffraction (XRD) measurements were made with X-ray diffractometer (D8-Advance), using Cu Kα (λ=1.5418 Å) as radiation source from 10° to 80° at the rate of 2° min^{-1}, the interlayer spacing was determined by (002) diffraction peaks, calculated by Scherrer equation Raman analysis was performed on a Labram-010 spectrograph, Nitrogen adsorption isotherms were carried on a tri-star-3020 at 77K after being degassed at 180 ℃ for 8 h and the surface area were calculated with the Brunauer-Emmett-Teller (BET) equation.

2.3. Measurement of anode performance

The working electrode of the carbonaceous materials were made by the HC powder (80 wt.%) with acetylene black (10 wt.%) and polyvinylidene difluoride (PVDF, 10 wt.%) dissolved in 1-methyl-2-pyrrolidione (NMP). Then mixed slurries were coated onto copper foil and cut into a disk with a diameter of 14 mm, the active materials mass on every electrode was about 2 mg. After drying under vacuum for 12 h at 110 ℃, the coin-type cells (2016-type) were assembled in an Ar-filled glove box, in which metallic Li was used as the counter electrode.1 M $LiPF_6$ dissolved in EC/DEC (1:1, v/v) as the electrolyte and polyethylene film as the separator.

The charge and discharge test of half cells were performed on a Land battery test system (LAND CT2001A) in a range of 0 V to 3 V with the current density from 50 mA g^{-1} to 1000 mA g^{-1}. The cyclic voltage (CV) measurement and electrochemical impedance spectroscopy (EIS) measurements were performed by CHI660E electrochemical workstation. The CV was performed under a scanning rate of 0.1 mV s^{-1} with a voltage window of 0-3 V and the EIS was performed with the frequency range of 100 KHZ-0.01 KHZ.

3. RESULTS AND DISCUSSION

Figure 1 shows the morphologies of all samples. Apparently, the morphologies of HCs derived from phenolic resin with different type and molecular weight are similar. It can be seen from the figure that all the HCs particles have the same average diameter of about 1μm, which are irregular with glossy surface as well as no porosity is observed.

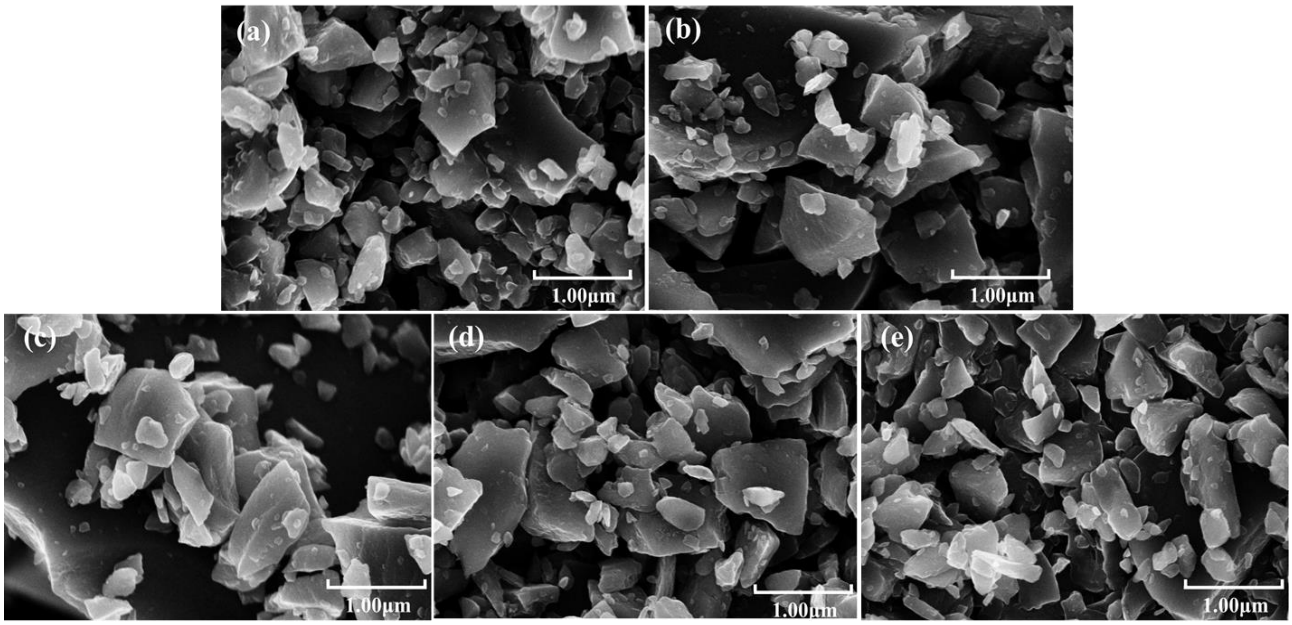

Figure 1. the SEM images of (a)MNHC, (b)HNHC, (c)LRHC, (d)MRHC and (e)HRHC

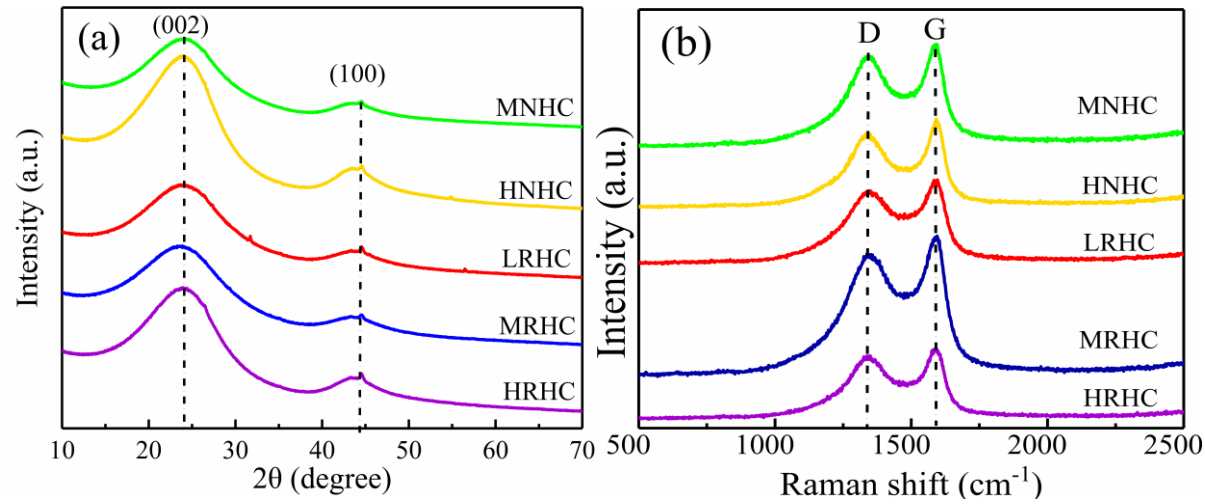

Figure 2. (a) XRD pattern at the degree of 10-80°; (b) Raman spectra of all hard carbon materials

The XRD patterns of HCs are displayed in the fig. 2(a), which are typical disordered carbon. The two broad and low-intensity peaks located around 24° and 45° are correlated to (002) and (100) diffraction peaks, respectively. The relatively obvious (002) diffraction peak is correlated to graphene-like layer structure, while the week (100) peak of the prepared samples are related to disordered or amorphous carbon [17,18]. It can be observed that the (002) diffraction peaks of the as-obtained HCs become sharp as the phenolic resin molecular weight increases for both type phenolic resin, it indicates that the graphitic crystallites are composed with more graphene layers, and may imply a higher conductivity. D_{002} values of the HC samples are summarized in Table 1. The interface spacings range from 3.70 to 3.76 Å, which are higher than that of graphite (3.34 Å), created favorable conditions for rapid insertion and de-insertion of lithium ions, and resulted in a better rate performance.

Obviously, the interlayer spacing (d_{002}) of HCs increases with the decreasing of molecular weight for Novolak-type phenolic resin, but it is opposite for Resole-type.

Raman spectroscopy is an especially useful technique which is widely used to explore the crystalline ordering of carbonaceous materials. Raman spectra of the as prepared HCs are presented in fig. 2(b). There are two peaks around 1335 cm^{-1} (D-band) and 1585 cm^{-1}(G-band) has been observed for all HC samples, and the peaks are broad and overlapping which revealed the defects and disordered structural characteristic. The two peaks are correlated to the vibrational mode of a tetrahedral sp3 configuration and a radial C-C stretching mode of sp^2-bonded carbon, respectively. The *ID/IG* values indicated the ratio of atomic defect among the carbon layer surface, HCs with higher *ID/IG* value revealed that the more defective and disordered structural characteristic of the samples. *ID/IG* values of HCs are summarized in Table 1, and the values shows the fellow order: MNHC<HNHC<HRHC<MRHC=LRHC. Atomic defect in the HC is one kind of active site for storing Li ion when HC as anode for LIB. Therefore, the capacity of hard carbon will improve with the increase of defect and disorder. The *ID/IG* values of LRHC and MRHC is higher than that of other HCs derived from the two types phenolic resin. As consequence, it may be expected that the capacity of LRHC and MRHC is higher, too, which will be examined in the following section.

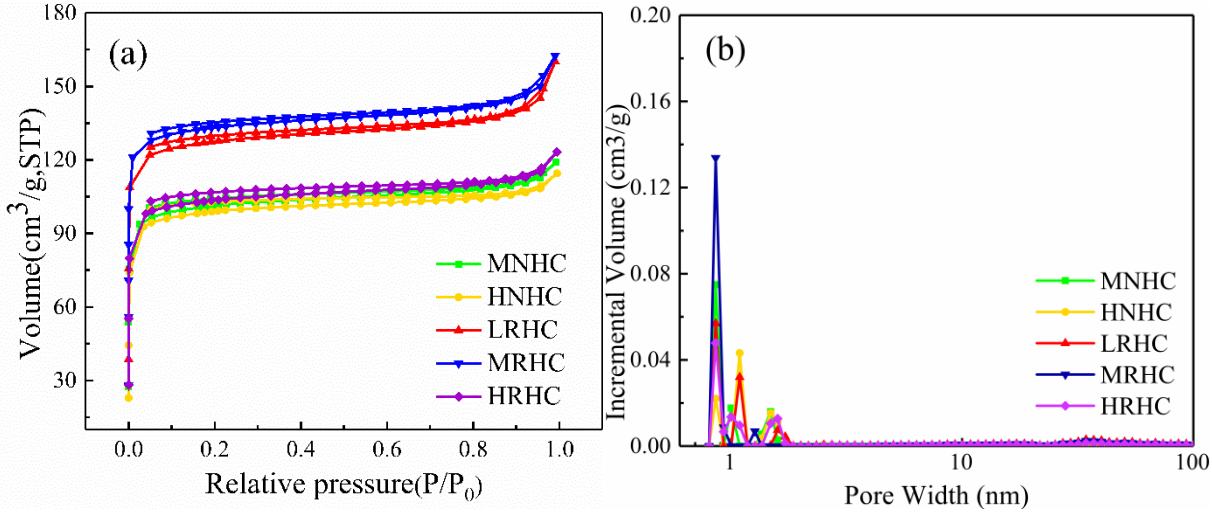

Figure 3. (a) Nitrogen adsorption-desorption isotherms at 77 K and (b) pore size distributions of HCs

Table 1. structural characteristics of the HCs

Sample	D_{002} (Å)	*ID/IG*	S_{BET} ($m^2\ g^{-1}$)
MNHC	3.70	2.2	356.1
HNHC	3.75	2.3	348.3
LRHC	3.76	2.7	364.0
MRHC	3.73	2.7	471.5
HRHC	3.71	2.4	449.0

The N_2 adsorption-desorption isotherms is shown in Fig. 3(a). The observed isotherms are of the

type I, revealing that large quantities of micropores are distributed within the HCs. BET surface areas of the HCs are summarized in Table 1. However, the specific surface areas of HCs derived from Resole-type phenolic resin is larger than that of Novolak-type, which exceed 300 $m^2 g^{-1}$, the large specific surface area enlarges the contact area between anode material and electrolyte, lead to form more SEI film, resulting in lower initial coulombic efficiency. According to the test report and calculate results, the DFT pore-size distributions is show in fig.3(b), It is noted that the pore size ranges from 0.75-3 nm, and the micropores around 0.85 nm and 1.3 nm are prominent for all of the HCs.

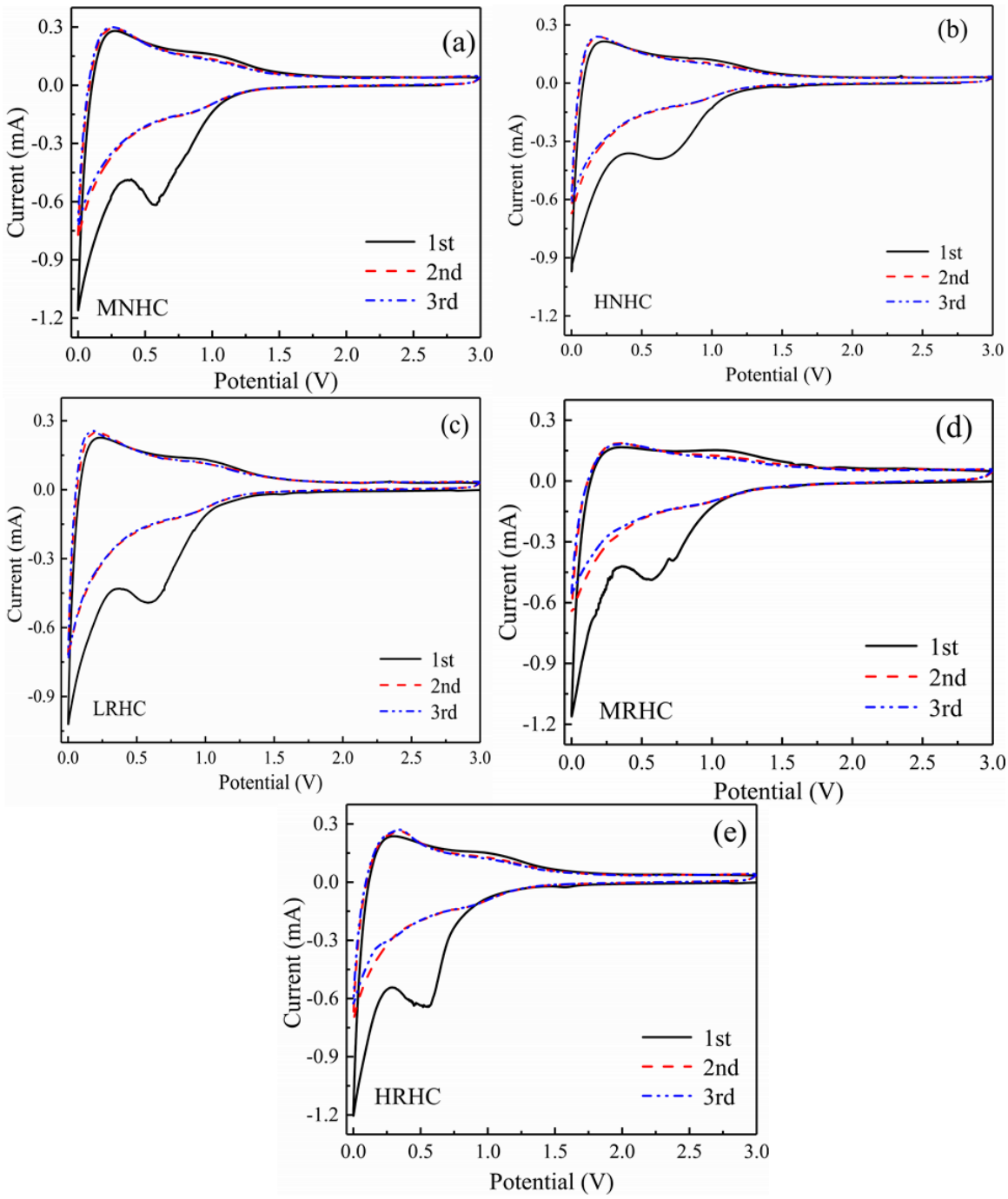

Figure 4. CV curves for the first three cycles between the voltage 0-3 V of (a)MNHC, (b)HNHC, (c)LRHC (d)MRHC and (e)HRHC

Table 2. Charge capacities, discharge capacities and coulomb efficiency in initial cycle of all samples

Sample	Charge capacity (mA h g^{-1})	Discharge capacity (mA h g^{-1})	Coulomb efficiency (%)
MNHC	470.9	955.4	49.3
HNHC	495.7	996.3	49.8
LRHC	606.2	1098.2	55.2
MRHC	564.2	1060.3	53.2
HRHC	466.7	926.3	50.4

These micropores are conducive to lithium ions storage and capacity improvement. Compared with other HCs, LRHC has relatively increased mesopores. Micropore and mesopore in hard carbon play an effective role as reservoir for lithium ion storage, they provide more advantageous way for rapid electrolyte transfer, which is very important for the rapid penetration and diffusion of Li ions.

The type and molecular weight of phenolic resin govern the structural characteristics and electrochemical performances of HCs prepared from phenolic resin. To confirm this, we evaluated the electrochemical performance of all samples by electrochemical testing of coin half-cells. Cyclic voltammograms (CVs) of the various HCs in the first three cycles with the sweep rate of 0.1 mV s^{-1} between 0-3 V are shown in Fig. 4. The cathodic peak at ca. 0.6 V during the first discharge process but disappeared in the subsequent cycles corresponds to irreversible reactions such as the formation of SEI film and the reactions of lithium ion with surface functional groups. The cathodic peak near 0 V correspond to the Li ion adsorption and intercalation in both sides of carbon sheets or walls of nanopores, and the anodic peak at ca. 0.2 V corresponds to the Li ion desorption and deintercalation from the HCs texture. After the first cycle, the CV curves of all HCs samples are similar.

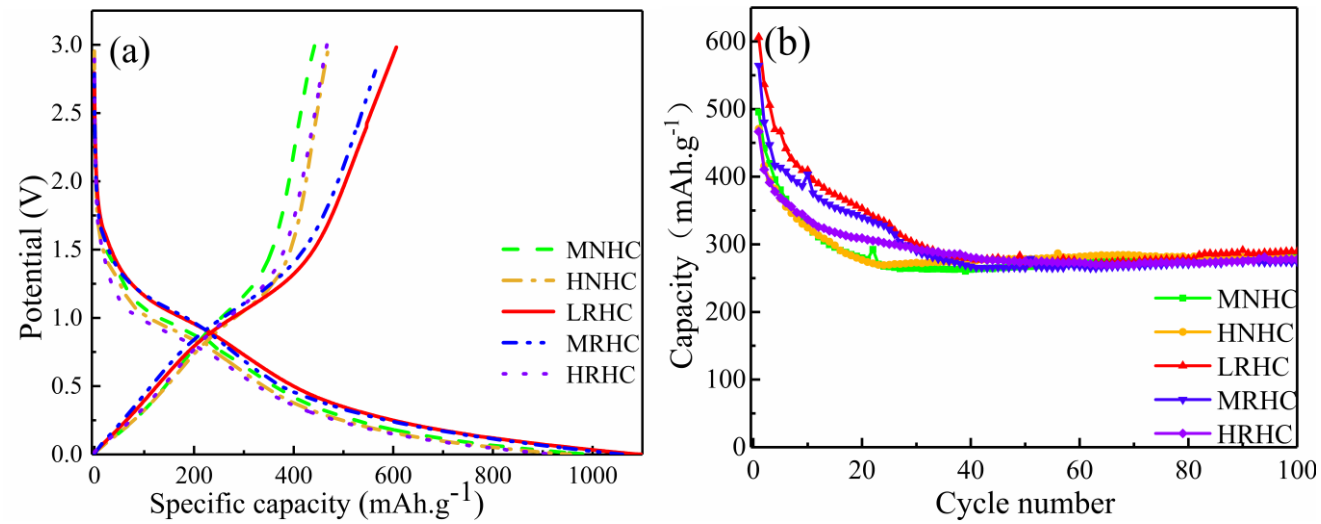

Figure 5. (a)charge/discharge profiles of the first cycle and (b) cycling stability at current density of 50 mA g^{-1}

Fig. 5(a) shows the first charge/discharge curves of various HCs electrodes at a current density of 50 mA g^{-1}. The initial coulomb efficiency of all samples is relatively low, these characteristics are in

Fline with the features of carbon anode heat-treated below 1000 ℃ [23,24]. Both of the HCs show similar voltage profiles and represent the sloped voltage profiles with high voltage hysteresis due to hydrogen residue [25,26]. Apparently, HCs derived from Resole-type phenolic resin demonstrate higher capacity than Novolak-type phenolic resin-based HCs except HRHC. Among them, LRHC represents the highest discharge capacity, and the discharge capacity of HCs increases with the decreasing molecular weight for resole-type phenolic resin. However, this is the opposite for Novolak-type phenolic resin. The relevant data of the first charge/discharge process are presented in Table 2. The initial discharge capacities of MNHC, HNHC, LRHC, MRHC and HRHC are 955.4, 996.3, 1098.2, 1060.3 and 926.3 mA h g^{-1}, and charge capacities are 470.9, 495.7, 606.2, 564.2 and 466.7 mA h g^{-1}, the corresponding coulomb efficiency are 49.3%, 49.8%, 55.2%, 53.2% and 50.4%, respectively. The LRHC represents the highest initial coulombic efficiency (55.2%) because of its highest discharge capacity (606.2 mA h g^{-1}) and relatively low specific surface area (364 m^2 g^{-1}). However, because of the large initial irreversible capacity loss, both HCs exhibited a low initial coulombic efficiency.

The irreversible capacity in the first cycle is usually caused by the following reasons: (I) the electrolyte decomposed on the negative electrode surface and formation of the SEI layer; (II) irreversible reactions between Li ions and heteroatoms or hydroxyl groups; (III) underpotential deposition of lithium at low voltage. According to the voltage range of the initial charge-discharge process, the irreversible capacity mainly attributed to the high specific surface area, extensively micropore structure and defects of hard carbon.

Fig. 5(b) shows the cyclic performance of HCs at the current density of 50 mA g^{-1}. In the figure, a continuous capacity decay in the first 30 cycles for all samples has been observed. This initial capacity losses due not only to the formation of SEI, but also to the underpotential deposition of Lithium metal occurs into the micropores. After 100 cycles, MNHC, HNHC, LRHC, MRHC and HRHC still maintained 57.5%, 59.2%, 47.7%, 48.6% and 59.5% of the initial discharge capacity, respectively.

Table 3. Comparing the capacity of hard carbon anode with other precursors

The precursor of HC	Pyrolysis temperature (℃)	Initial charge capacity (mA h g^{-1})	Ref.
polyacrylonitrile	600	426 at 0.2 mA cm^{-2}	[19]
oxidized pitch	1000	440 at 18.6 mA g^{-1}	[20]
anthracite	1100	370 at 30 mA g^{-1}	[21]
needle coke	2800	477 at 50 mA g^{-1}	[22]
phenolic resin (LRR)	800	606 at 50 mA g^{-1}	This work

Table. 3 is a comparison of the hard carbon prepared by different precursors in this work and other references. Obviously, low molecular weight Resole-type phenolic resin has a great advantage in capacity as hard carbon precursor. In addition, low carbonization temperature also makes it possible to reduce costs and conducive to large-scale production.

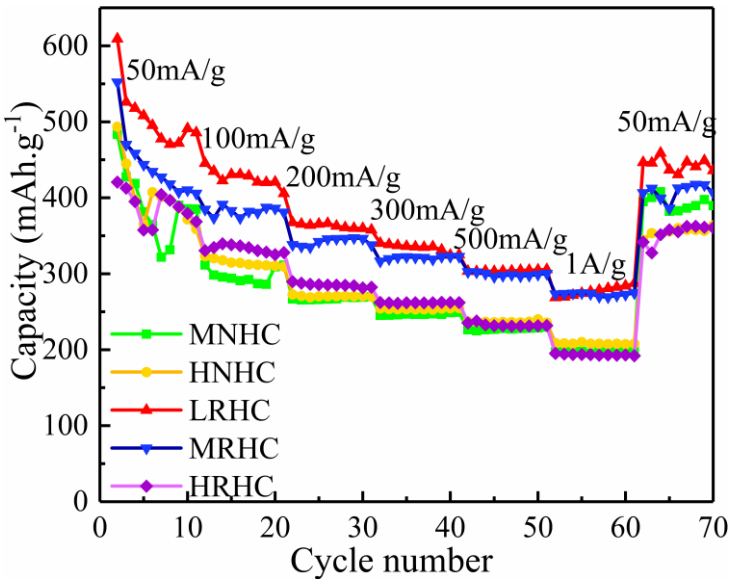

Figure 6. Rate capability test at different current density of HCs

Fig.6 shows the rate performance of the HCs samples, with a charged/discharged current density range from 50 to 1000 mA g^{-1}. It is clear that LRHC exhibits the highest reversible capacities due to the high interlayer spacing and unique pore distribution. The capacity of LRHC decreases to 450 mA h g^{-1}, 360 mA h g^{-1}, 340 mA h g^{-1}, 300 mA h g^{-1} and 270 mA h g^{-1} respectively with the increase of current density. Apparently, HCs derived from Resole-type phenolic resin delivered better rate capacity than that of Novolak-type phenolic resin-based HCs except HRHC, and the rate capacity decreases with the increasing molecular weight for resole-type phenolic resin.

4. CONCLUSION

In the present work, the structural characteristic and electrochemical performance of HCs prepared from phenolic resin with different type and molecular weight were measured. The interlayer spacing of HCs increases with the decreasing molecular weight for resole-type phenolic resin, but it is opposite for Resole-type. Higher interlayer spacing indicates better rate performance, and LRHC exhibited the best rate performance. The *ID/IG* values of LRHC and MRHC is higher than that of other HCs derived from the two types phenolic resin, and high *ID/IG* values indicated more active site for lithium ion storage. The specific surface areas of HCs derived from Resole-type phenolic resin is larger than that of Novolak-type. However, compared with other HCs, LRHC has more mesopores; they provide an advantageous way for the rapid transfer of electrolytes and greatly improve the rapid transport of Li-ion. HCs derived from Novolak-type phenolic resin usually showed poorer rate performance and lower reversible capacity than that of Resole-type phenolic resin-based HCs. LRHC displayed the best electrochemical performance, with the highest reversible capacity (606.2 mA h g^{-1}), initial Coulombic efficiency (55.2%), and rate capacity. In summary, when phenolic resin precursors are used to fabricate HC anode for Li-ion battery, the resole-type phenolic resin with low molecular weight is the best candidate.

ACKNOWLEDGEMENTS
This work was supported by National Natural Science Foundation of China (Grant No. 51772083), Major Special Plan for Science and Technology in Hunan Province (No. 2018GK1030), New Strategic Plan of Hunan Province Special Project on Science and Technology Tackling of Emerging Industries and Transforming Major Achievement (No. 2018GK4011).

References

1. J.R. Dahn, Z. Tao, Y. Liu and J.S. Xue, *Science*, 270 (1995) 590.
2. J.R. Dahn, W. Xing and Y. Gao, *Carbon*, 35 (1997) 825.
3. Y.S. Han, J.S. Yu, G.S. Park and J.Y. Lee, *J. Electrochem. Soc*, 146 (1999) 3999.
4. J.S. Wainright, C.A. Zorman, *J. Electrochem. Soc*, 142 (1995) 379.
5. Y. Liu, Xue, T. Zheng and J.R. Dahn, *Carbon*, 34 (1996) 193.
6. W. Xing, J.S. Xue, T. Zheng, A. Gibaud and J.R. Dahn, *J. Electrochem. Soc*, 143 (1996) 3482.
7. H. Zhang, W. Zhang, H. Ming, J. Pang, H. Zhang, G. Cao and Y. Yang, *Chem. Eng. J.*, 341 (2018) 280.
8. C.W. Park, S.H. Yoon, I.L. Sang and S.M. Oh, *Carbon*, 38 (2000) 995.
9. J. Wang, J.L. Liu, Y.G. Wang, C.X. Wang and Y.Y. Xia, *Electrochimica Acta*, 74 (2012) 1.
10. L. Elmira Memarzadeh, D. Jia, C. Kai, K. Alireza, K. W Peter, H. Michael and M. David, *Acs Nano*, 8 (2015) 7115.
11. W. Lv, F. Wen, J. Xiang, Z. Jing, L. Lei, L. Wang, Z. Liu and Y. Tian, *Electrochimica Acta*, 176 (2015) 533.
12. L. Bei, X. Zhou, H. Chen, Y. Liu and H. Li, *Electrochimica Acta*, 208 (2016) 55.
13. J. Ou, Y. Zhang, L. Chen, Q. Zhao, Y. Meng, Y. Guo and D. Xiao, *J. Mater. Chem. A.*, 3 (2015) 6534.
14. X. Hao, W. Jie, D. Bing, Y. Wang, C. Zhi, D. Hui and X. Zhang, *J. Power Sources.*, 352 (2017) 34.
15. H. Yang, Z. Lin, M. Zheng, T. Wang, J. Yang, F. Yuan, X. Lu, L. Lin and D. Sun, *J. Power Sources.*, 307 (2016) 649.
16. Y. Jin, K. Tian, W. Lu, X. Zhang and G. Xin, *J. Mater. Chem. A.*, 4 (2016) 15968.
17. N.I. Jiangfeng, Y. Huang and L. Gao, *J. Power Sources.*, 223 (2013) 306.
18. J.L. Liu, J. Wang and Y.Y. Xia, *Electrochimica Acta*, 56 (2011) 7392.
19. Y. Wu, S. Fang and Y. Jiang, *J. Power Sources*, 75 (1998) 201.
20. A. Piotrowska, K. Kierzek, P. Rutkowski and J. Machnikowski, *J. Anal. Appl. Pyrol*, 102 (2013) 1.
21. Y.J. Kim, H. Yang, S.H. Yoon, Y. Korai and I. Mochida, *J. Power Sources*, 113 (2003) 157.
22. W. Ren, Z. Zhang, Y. Wang, G. Kan, Q. Tan, Z. Zhong and F. Su, *RSC Adv*, 5 (2015) 11115.
23. A. Mabuchi, K. Tokumitsu, H. Fujimoto and T. Kasuh, *J. Electrochem. Soc.*, 142 (1995) 1041.
24. K. Sawai, Y. Iwakoshi, and T. Ohzuku, *Solid State Ion*, 69 (1994) 273.
25. E. Buiel and J.R. Dahn, *Electrochimica Acta*, 45 (1999) 121.
26. K. Gotoh, M. Maeda, A. Nagai, A. Goto, M. Tansho, K. Hashi, T. Shimizu and H. Ishida, *J. Power Sources*, 162 (2006) 1322.